Theranostics Targeting Fibroblast Activation Protein in the Tumor Stroma: ^{64}Cu- and ^{225}Ac-Labeled FAPI-04 in Pancreatic Cancer Xenograft Mouse Models

Tadashi Watabe[1,2], Yuwei Liu[1], Kazuko Kaneda-Nakashima[2,3], Yoshifumi Shirakami[2], Thomas Lindner[4], Kazuhiro Ooe[1,2], Atsushi Toyoshima[2,3], Kojiro Nagata[5], Eku Shimosegawa[2,6], Uwe Haberkorn[4,7,8], Clemens Kratochwil[4], Atsushi Shinohara[2,9], Frederik Giesel[2,4], and Jun Hatazawa[2,10]

[1]Department of Nuclear Medicine and Tracer Kinetics, Graduate School of Medicine, Osaka University, Osaka, Japan; [2]Institute for Radiation Sciences, Osaka University, Osaka, Japan; [3]Core for Medicine and Science Collaborative Research and Education, Project Research Center for Fundamental Sciences, Graduate School of Science, Osaka University, Osaka, Japan; [4]Department of Nuclear Medicine, University Hospital Heidelberg, Heidelberg, Germany; [5]Radioisotope Research Center, Institute for Radiation Sciences, Osaka University, Osaka, Japan; [6]Department of Molecular Imaging in Medicine, Graduate School of Medicine, Osaka University, Osaka, Japan; [7]Clinical Cooperation Unit of Nuclear Medicine, DKFZ, Heidelberg, Germany; [8]Translational Lung Research Center Heidelberg, German Center for Lung Research (DZL), Heidelberg, Germany; [9]Department of Chemistry, Graduate School of Science, Osaka University, Osaka, Japan; and [10]Research Center for Nuclear Physics, Osaka University, Osaka, Japan

Fibroblast activation protein (FAP), which promotes tumor growth and progression, is overexpressed in cancer-associated fibroblasts of many human epithelial cancers. Because of its low expression in normal organs, FAP is an excellent target for theranostics. In this study, we used radionuclides with relatively long half-lives, ^{64}Cu (half-life, 12.7 h) and ^{225}Ac (half-life, 10 d), to label FAP inhibitors (FAPIs) in mice with human pancreatic cancer xenografts. **Methods:** Male nude mice (body weight, 22.5 ± 1.2 g) were subcutaneously injected with human pancreatic cancer cells (PANC-1, n = 12; MIA PaCa-2, n = 8). Tumor xenograft mice were investigated after the intravenous injection of ^{64}Cu-FAPI-04 (7.21 ± 0.46 MBq) by dynamic and delayed PET scans (2.5 h after injection). Static scans 1 h after the injection of ^{68}Ga-FAPI-04 (3.6 ± 1.4 MBq) were also acquired for comparisons using the same cohort of mice (n = 8). Immunohistochemical staining was performed to confirm FAP expression in tumor xenografts using an FAP-α-antibody. For radioligand therapy, ^{225}Ac-FAPI-04 (34 kBq) was injected into PANC-1 xenograft mice (n = 6). Tumor size was monitored and compared with that of control mice (n = 6). **Results:** Dynamic imaging of ^{64}Cu-FAPI-04 showed rapid clearance through the kidneys and slow washout from tumors. Delayed PET imaging of ^{64}Cu-FAPI-04 showed mild uptake in tumors and relatively high uptake in the liver and intestine. Accumulation levels in the tumor or normal organs were significantly higher for ^{64}Cu-FAPI-04 than for ^{68}Ga-FAPI-04, except in the heart, and excretion in the urine was higher for ^{68}Ga-FAPI-04 than for ^{64}Cu-FAPI-04. Immunohistochemical staining revealed abundant FAP expression in the stroma of xenografts. ^{225}Ac-FAPI-04 injection showed significant tumor growth suppression in the PANC-1 xenograft mice, compared with the control mice, without a significant change in body weight. **Conclusion:** This proof-of-concept study showed that ^{64}Cu-FAPI-04 and ^{225}Ac-FAPI-04 could be used in theranostics for the treatment of FAP-expressing pancreatic cancer. α-therapy targeting FAP in the cancer stroma is effective and will contribute to the development of a new treatment strategy.

For correspondence and reprints contact: Tadashi Watabe, Osaka University, 2-2 Yamadaoka, Suita, Osaka 565-0871 Japan.
E-mail: watabe@tracer.med.osaka-u.ac.jp
Published online Oct. 4, 2019.

Key Words: theranostics; fibroblast activation protein; pancreatic cancer; α-therapy; actinium

J Nucl Med 2020; 61:563–569
DOI: 10.2967/jnumed.119.233122

In targeted α-therapy and theranostics, cancer-specific biomarkers, such as prostate-specific membrane antigen for prostate cancer (*1,2*), have limited expression in other cancer types and therefore are not generalizable for the development of a universal cancer therapy. The tumor microenvironment (stroma), which consists of nonmalignant cells such as macrophages, fibroblasts, endothelial cells, and others, appears as a novel and promising target. In the stroma, cancer-associated fibroblasts are crucial components that stimulate cancer cell growth and invasion (*3–5*). Fibroblast activation protein (FAP), which promotes tumor growth and progression, is overexpressed in cancer-associated fibroblasts of many human epithelial cancers (*6*). FAP expression also correlates with prognosis (*7*). Since it is expressed at low levels in normal tissues, FAP is an excellent target for theranostics in oncology. Recently, small-molecule FAP inhibitor (FAPI) probes were developed (*8–10*), and the diagnostic utility of ^{68}Ga-FAPI PET has been established in various cancer types, demonstrating rapid distribution at the target site and minimal uptake in normal organs (*11,12*). In addition, Loktev et al. successfully increased FAP binding and improved pharmacokinetics by chemical modification of the FAPI probes (*10*). They also reported high uptake of ^{177}Lu-labeled FAPI derivatives in HT-1080-FAP tumor–bearing mice. However, the efficacy of α-emitters targeting FAP remains unknown. In this study, we used radionuclides with longer half-lives, ^{64}Cu (half-life, 12.7 h) and ^{225}Ac (half-life, 10 d), to label FAPI for evaluation of tumor uptake in the delayed phase after injection. The purpose of this study was to evaluate the biodistribution and treatment effect of ^{225}Ac-labeled and ^{64}Cu-labeled FAPI in FAP-positive human pancreatic cancer xenografts.

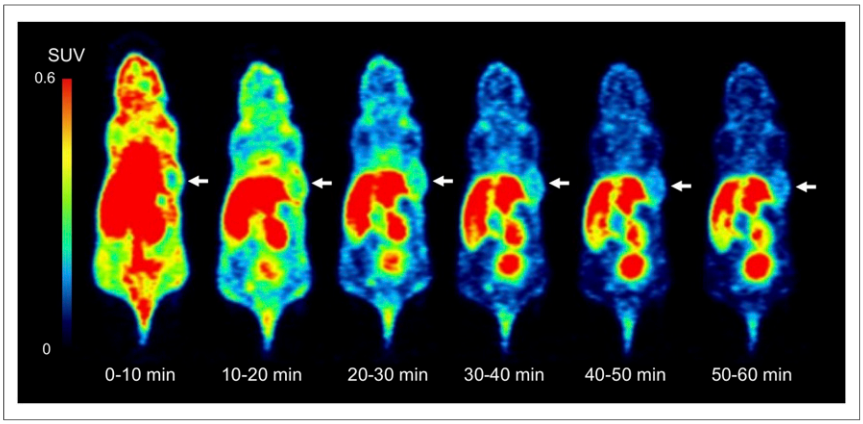

FIGURE 1. Dynamic PET imaging of ^{64}Cu-FAPI-04 in PANC-1 xenograft model (arrows indicate tumor xenograft).

MATERIALS AND METHODS

Preparation of ^{64}Cu-, ^{68}Ga-, and ^{225}Ac-Labeled FAPI-04 Solutions

The FAPI-04 precursor was obtained from Heidelberg University on the basis of a material transfer agreement for collaborative research. $^{64}CuCl_2$ dissolved in 0.1 M hydrochloride was purchased from Fuji Film Toyama Chemicals. In a micro tube, the $^{64}CuCl_2$ solution (74 MBq, 0.035 mL), 0.2 M ammonium acetate (0.47 mL), 2% sodium ascorbate (0.5 mL), and 1 mM FAP-04 (0.028 mL) were added and reacted at 80°C for 1 h. A ^{68}Ge–^{68}Ga generator was purchased from iTG Isotope Technologies Garching GmbH. ^{68}Ga was eluted with a solution of 0.1 M hydrochloride from the generator. In a micro tube, the ^{68}Ga solution (64 MBq), 2.5 M sodium acetate (0.03 mL), 10% ascorbic acid (0.02 mL), and 1 mM FAPI-04 (0.03 mL) were added and reacted at 95°C for 20 min.

^{225}Ac was obtained by milking from its grandparent nuclide ^{229}Th via ^{225}Ra (*13*). A dry residue containing ^{229}Th and its descendant nuclides was dissolved with 8 M HNO_3 (0.5 mL) and was loaded onto 2 connected anion-exchange columns (Muromac 1 × 8, 100–200 mesh, NO_3^- form, ~1-mL column volume). Then, 8 M HNO_3 (3 mL) was loaded onto the columns to elute ^{225}Ra and ^{225}Ac. For only the bottom column, 8 M HNO_3 (3 mL) was additionally loaded to completely strip ^{225}Ra and ^{225}Ac. ^{229}Th on the top column was separately recovered with 2 M HCl (10 mL) and distilled water (5 mL). The 8 M HNO_3 effluent was diluted to 4 M HNO_3 and loaded onto a column filled with *N,N,N′,N′*-tetrakis-2-ethylhexyldiglycolamide branched resin (2-mL cartridge; Eichrom). After ^{225}Ra was eluted with 4 M HNO_3 (6 mL), ^{225}Ac was stripped with 0.05 M HNO_3 (10 mL). After evaporation to dryness, ^{225}Ac was dissolved in a 0.2 M ammonium acetate solution (0.2 mL). The radioactivity of ^{225}Ac was determined from the γ-ray emissions for ^{221}Fr (218 keV) and ^{213}Bi (440 keV), which were in radioactive secular equilibrium with its parent ^{225}Ac, using a high-purity germanium detector (BE-2020; Canberra). In a micro tube, the ^{225}Ac solution (130 kBq, 0.2 mL), 0.2 M ammonium acetate (0.1 mL), 7% sodium ascorbate (0.1 mL), and 1 mM FAPI-04 (0.3 mL) were added and reacted at 80°C for 2 h.

Radiochemical yields for the 3 products labeled with ^{64}Cu, ^{68}Ga, and ^{225}Ac were analyzed by cellulose acetate electrophoresis. An aliquot of each product was spotted on a strip of cellulose acetate. The voltage applied to the strip was 133 V at 1 mA/cm in a solution of 0.06 M barbital buffer (pH 8.6) for 40 min. The strip was exposed to an imaging plate, and the radioactivity on the strip was analyzed using a bioimager (Typhoon7000; GE Healthcare). The radiochemical yields of ^{64}Cu-FAPI-04, ^{68}Ga-FAPI-04, and ^{225}Ac-FAPI-04 were 85.0%–88.5%, 95.0%, and 94.7%–96.9%, respectively.

Preparation of Xenograft Models

PANC-1 and MIA PaCa-2 cells were obtained from American Type Culture Collection. The cells were maintained in culture medium (RPMI1640 with L-glutamine and phenol red [Fujifilm Wako Pure Chemical] for PANC-1 and Dulbecco modified Eagle medium [high glucose] with L-glutamine and phenol red for MIA PaCa-2) with 10% heat-inactivated fetal bovine serum and 1% penicillin-streptomycin. Male nude mice were purchased from Japan SLC Inc.. Animals were housed under a 12-h-light/12-h-dark cycle and given free access to food and water. Tumor xenograft models were established by the subcutaneous injection of human pancreatic cancer cells (PANC-1 or MIA PaCa-2, 1×10^7 cells) suspended in 0.1 mL of phosphate-buffered saline and Matrigel (1:1; BD Biosciences) in nude mice ($n = 20$). All animal experiments were performed in compliance with the guidelines of the Institute of Experimental Animal Sciences. The protocol was approved by the Animal Care and Use Committee of the Osaka

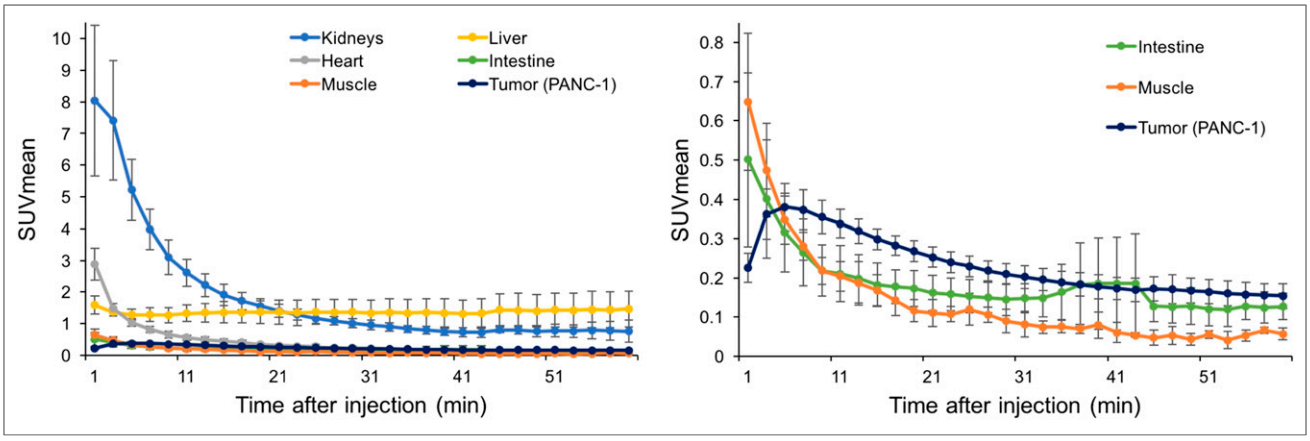

FIGURE 2. Time–activity curve for PANC-1 tumor and normal organs on ^{64}Cu-FAPI-04 PET. (Note that vertical scales in left and right panels are different.)

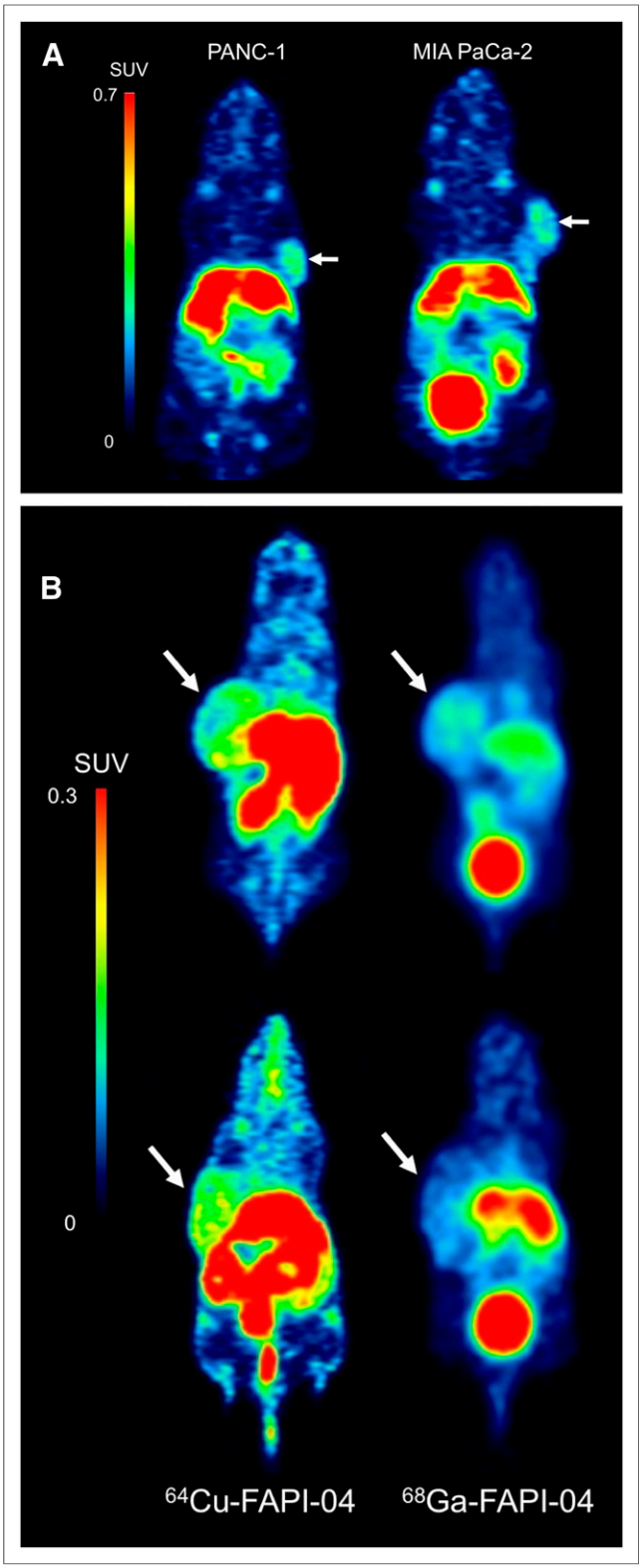

FIGURE 3. (A) Delayed PET imaging of ^{64}Cu-FAPI-04 (2.5 h after injection) in PANC-1 and MIA PaCa-2 xenograft models. (B) Comparison of uptake rates between ^{64}Cu-FAPI-04 (2.5 h after injection) and ^{68}Ga-FAPI-04 (1 h after injection) (top, PANC-1; bottom, MIA PaCa-2).

University Graduate School of Medicine. The criteria for euthanasia were as follows: first, animal showed signs of intolerable suffering; second, a significant decrease in activity or a marked decrease in food and water intake was observed; third, the tumor size reached 3 cm in diameter; and fourth, the observation period ended (after 51 d). Euthanasia was performed by deep anesthesia by isoflurane inhalation.

^{64}Cu-FAPI-04 PET Imaging and Analysis

Tumor xenograft mice (9 wk old; body weight, 22.5 ± 1.2 g) were investigated using a small-animal PET scanner (Siemens Inveon PET/CT) 3 wk after the implantation of PANC-1 (n = 12) and MIA PaCa-2 (n = 8) when tumor size reached approximately 1.2 cm in diameter (*14*). After the intravenous injection of ^{64}Cu-FAPI-04 (7.21 ± 0.46 MBq), dynamic scans (scan duration, 60 min) were acquired for PANC-1 mice (n = 4) and delayed PET scans (scan duration, 20 min) were acquired 2.5 h after injection for all mice (n = 20) under isoflurane anesthesia. Sinograms were generated in multiple time-frames in the dynamic PET scan (2 min × 30 frames) and in 1 frame in the delayed PET scan. All PET data were reconstructed by 2-dimensional ordered-subset expectation maximization (16 subsets, 4 iterations) with attenuation and scatter correction. Regional uptake of radioactivity was decay-corrected to the injection time and expressed as the SUV, which was corrected for the dose (MBq) and body weight (g). Ellipsoid sphere regions of interest were manually placed on the tumor, muscle, heart, liver, intestine, kidneys, and bladder of PET images with reference to the fused PET/CT images. SUV_{mean} was measured to obtain time–activity curves and static uptake in the delayed scan using PMOD (version 3.6).

Comparison of Uptake Between ^{64}Cu-FAPI-04 and ^{68}Ga-FAPI-04

Static scans 1 h after the injection of ^{68}Ga-FAPI-04 (3.6 ± 1.4 MBq) were performed using the same cohort of xenograft mice. Uptake rates were compared between ^{64}Cu-FAPI-04 and ^{68}Ga-FAPI-04 using PANC-1 or MIA PaCa-2 xenograft mice (n = 4 each).

Immunohistochemistry

Immunohistochemical staining was performed to confirm FAP expression in the tumor xenograft using a FAP-α antibody. After the animals were sacrificed by euthanasia, all tumor xenografts were resected and fixed with 4% paraformaldehyde (overnight, 4°C). The fixed tissues were immersed in 30% sucrose in phosphate-buffered saline (overnight, 4°C). Frozen sections of the samples were then incubated with anti-FAP, α-antibody (ab53066; Abcam). Immunohistochemistry was performed using the Dako EnVision + System–HRP Labeled Polymer Anti-Rabbit (K4003) (DAKO Corp.). Staining without the primary antibody was also performed to confirm its specificity as a negative control. The stained sections were analyzed by light microscopy (Keyence).

In Vitro Cellular Uptake Analysis

Cellular uptake was analyzed to confirm that the expression of FAP was not observed in the tumor cell itself but in the stroma of the tumor xenograft. C6 glioma cells were obtained from Riken BRC and used as a negative control for the FAP expression test. PANC-1 cells, MIA PaCa-2 cells, and C6 glioma cells were seeded onto 24-well plates (1×10^5 cells per well) and cultured overnight. ^{64}Cu-FAPI-04 solution (40 kBq/250 μL) was added to each well and incubated for 10 min. Cells were washed twice with phosphate-buffered saline and collected in solutions after they were lysed with 0.1 N NaOH. The radioactivity of the collected solution was measured by AccuFlex γ7000 (Hitachi Aloka). The amounts of proteins were measured in a plate reader (iMark; Bio-Rad) using the bicinchoninic acid protein assay kit (Fujifilm Wako Pure Chemical Corp.).

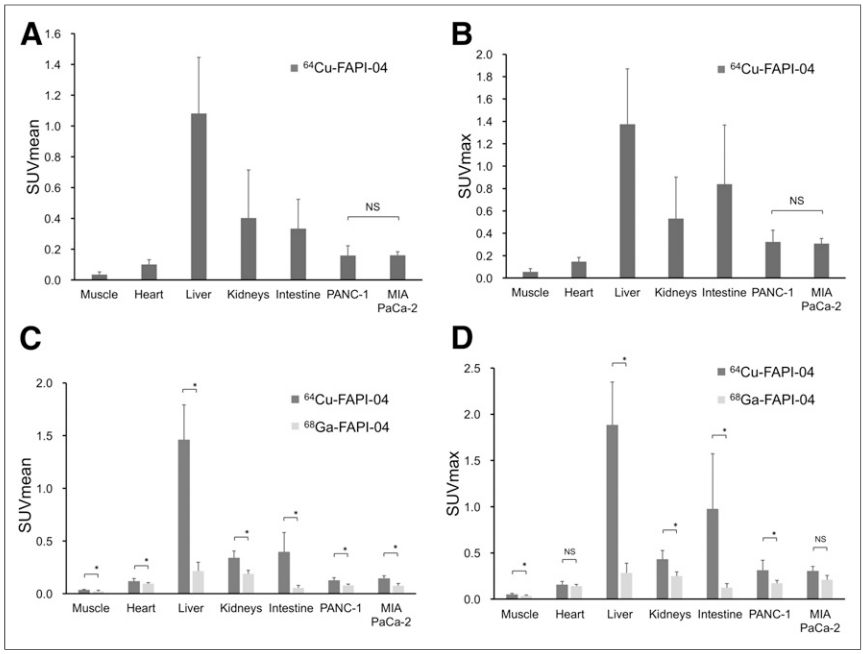

FIGURE 4. (A and B) Tracer uptake in tumor and normal organs on ^{64}Cu-FAPI-04 PET (2.5 h after injection). (C and D) Comparison of uptake rates in tumor and normal organs between ^{64}Cu-FAPI-04 and ^{68}Ga-FAPI-04 PET. *$P < 0.05$. NS = not significant.

Biodistribution and Treatment Effect of ^{225}Ac-FAPI-04

^{225}Ac-FAPI-04 (10 kBq) was injected into PANC-1 xenograft mice ($n = 6$, 3 wk after implantation; tumor size, 0.81 ± 0.27 cm^3) to evaluate the whole-body biodistribution. Animals were sacrificed by euthanasia at 3 and 24 h after injection, and samples of major organs were collected after dissection. For the bone and muscle, part of the rear limb was collected. For the collection of bone marrow, 0.8 mL of saline was used for flushing. The radioactivity of each sample was measured using a 2480 Wizard^2 γ-Counter (Perkin Elmer). Radioactivity counts were normalized by calibration using the ^{225}Ac standard solution. Excrement in the cage was also measured to calculate the excretion rate at 3 and 24 h after injection. At 3 h after injection, lung data were not available because of a technical problem. ICR mice (7 wk old, $n = 3$) were used as an alternative.

For radioligand therapy using an α-emitter, ^{225}Ac-FAPI-04 (34 kBq/100 μL) was injected into PANC-1 xenograft mice via the tail vein ($n = 6$, 3 wk after implantation; tumor size, 0.98 ± 0.66 cm^3). Tumor size was monitored by the elliptic sphere model calculation using the caliper and compared with that of control mice for up to 51 d ($n = 6$; tumor size at 3 wk after implantation, 0.85 ± 0.59 cm^3). The equivalent dose (Gy) in the dosimetry of ^{225}Ac was estimated according to a previous report (*15*). Residence times were calculated from the tumoral uptakes at 3 and 24 h after injection, and the area under the curve after 24 h was assumed to decrease with physical decay. Energy per decay (MeV/Bq·s) of ^{225}Ac was estimated as 28.0 from the α-particle energy and the recoil energy, including the emission from all daughter nuclides.

Statistical Analysis

Comparisons between 2 groups were performed using the Mann–Whitney *U* test and SPSS (version 25.0; IBM Corp.), and a *P* value of less than 0.05 indicated statistical significance.

RESULTS

Dynamic PET images of the ^{64}Cu-FAPI-04 in PANC-1 xenograft model are summarized in Figure 1. Rapid clearance through the kidneys and slow washout from the tumors were observed (Fig. 2). Delayed PET imaging of ^{64}Cu-FAPI-04 showed moderate uptake in the tumors and relatively high uptake in the liver and intestine (Fig. 3). The SUV_{mean} of delayed scans was 0.23 ± 0.07 in the PANC-1 xenograft, 0.17 ± 0.03 in the MIA PaCa-2 xenograft, 0.04 ± 0.03 in the muscle, 0.10 ± 0.03 in the heart, 0.91 ± 0.23 in the liver, 0.32 ± 0.17 in the intestine, 0.52 ± 0.48 in the kidneys, and 26.72 ± 31.11 in the bladder (Fig. 4A). Accumulation in the tumor or most of the normal organs was significantly higher for ^{64}Cu-FAPI-04 than for ^{68}Ga-FAPI-04, and excretion in the urine was higher for ^{68}Ga-FAPI-04 than for ^{64}Cu-FAPI-04 (Figs. 3B, 4C, and 4D). Immunohistochemical staining revealed abundant FAP expression in the stroma of both PANC-1 and MIA PaCa-2 xenografts (Fig. 5). In vitro cellular uptake analysis revealed minimal accumulation in the PANC-1 and MIA PaCa-2 tumor cells (Supplemental Fig. 1; supplemental materials are available at http://jnm.snmjournals.org). The biodistribution of ^{225}Ac-FAPI-04 is shown in Table 1. The

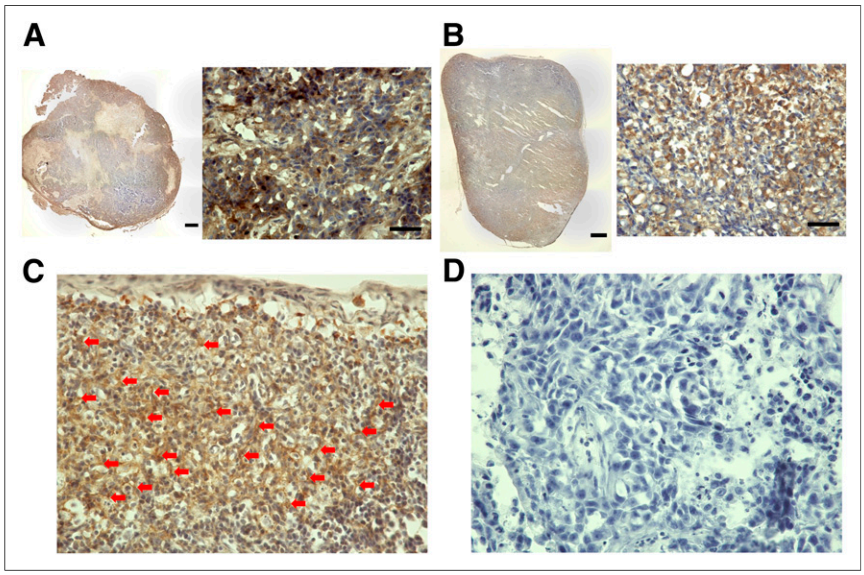

FIGURE 5. (A and B) Immunohistochemical staining of PANC-1 (A) and MIA PaCa-2 (B) tumor xenografts using FAP-α-antibody (left, low magnification [bar = 1,000 μm]; right, high magnification [bar = 50 μm]). (C) Positive-control staining of FAP in stroma of PANC-1 xenograft (arrows indicate stroma). (D) Negative-control staining in PANC-1 xenograft without primary antibody (high magnification).

liver, kidney, and tumor (PANC-1 xenograft) showed high uptake, although moderate washout from the tumor was observed between 3 and 24 h after injection. Excrement samples at 24 h were 91.2% ± 13.1% of the injected dose in urine and 2.10% ± 0.10% in feces. ^{225}Ac-FAPI-04 injection showed significant tumor growth suppression in the PANC-1 xenograft mice compared with the control mice, without a significant change in body weight (Fig. 6). The equivalent dose in the tumor was estimated to be 5.68 ± 0.77 Gy/MBq.

DISCUSSION

We evaluated FAP expression in human pancreatic cancer xenografts using ^{64}Cu-FAPI-04 PET with histologic confirmation and demonstrated the treatment effect of ^{225}Ac-FAPI-04. We have successfully proved the concept that α-therapy targeting FAP in the cancer stroma is effective.

FAP has been identified in a wide range of cancer types, such as breast cancer, colon cancer, pancreatic cancer, ovarian cancer, and hepatocellular carcinoma (*11,12*). It shows minimal expression in normal tissues. For targeted α-therapy, side effects associated with tracer accumulation in normal tissues may present a major issue. For example, side effects in the salivary gland (xerostomia) have been reported in association with physiologic accumulation for targeted α-therapy using ^{225}Ac-PSMA-617 (*1,16*). Therefore, the low FAP expression in normal tissues is a great advantage for targeted α-therapy using FAPI. Furthermore, most cancer therapies target markers of tumor cells; α-therapy targeting FAP is a new treatment option that can be used in combination with other therapies directly targeting cancer cells. Since the microenvironment in cancer is heterogeneous, combinations with other ligands that are internalized in tumor cells are an interesting strategy to irradiate the tumor by α-particles from both inside and outside cancer cells.

After the administration of ^{225}Ac-FAPI-04, necrotic collapse of the tumor xenograft, as revealed by a dark brown scab on the skin surface of the xenograft, was observed (Supplemental Fig. 2). We occasionally observed this phenomenon if the tumor reached a large size in control mice. However, mice treated with ^{225}Ac-FAPI-04 showed collapse at a much smaller tumor size (1.54 ± 0.65 cm^3), followed by shrinkage of the tumor around day 20. Extensive tumor necrosis has also been reported after treatment with molecular targeting drugs (*17,18*). The destruction of the cancer stroma may make it difficult to maintain the structure of the tumor mass because of the α-irradiation effect of ^{225}Ac-FAPI-04.

Both PANC-1 and MIA PaCa-2 cells are major cell lines of pancreatic ductal adenocarcinoma that reportedly harbor *KRAS* and *TP53* gene mutations and exhibit neuroendocrine differentiation (*19*). In cellular morphologic patterns, PANC-1 cells display a heterogeneous size population, whereas MIA PaCa-2 cells display relatively a homogeneous size. Regarding stromal cell composition, human pancreatic cancer samples show large, solid structures of stroma, whereas xenografts in mice display a relatively scattered stromal distribution (*20*), which is consistent with the present study.

TABLE 1
Whole-Body Distribution After Intravenous Administration of ^{225}Ac-FAPI-04 in PANC-1 Xenograft Model

	%ID		%ID/g	
Site	3 h	24 h	3 h	24 h
Brain	0.015 ± 0.004	0.004 ± 0.001	0.047 ± 0.007	0.015 ± 0.004
Submandibular gland	0.034 ± 0.004	0.010 ± 0.001	0.282 ± 0.059	0.083 ± 0.020
Heart	0.031 ± 0.005	0.001 ± 0.003	0.277 ± 0.041	0.013 ± 0.030
Lung	0.028 ± 0.008	0.008 ± 0.005	0.128 ± 0.032	0.041 ± 0.023
Liver	0.745 ± 0.005	0.443 ± 0.032	0.685 ± 0.042	0.374 ± 0.037
Stomach	0.028 ± 0.007	0.009 ± 0.004	0.224 ± 0.060	0.096 ± 0.042
Small intestine	0.229 ± 0.036	0.048 ± 0.008	0.275 ± 0.050	0.055 ± 0.003
Large intestine	0.025 ± 0.005	0.014 ± 0.003	0.434 ± 0.108	0.098 ± 0.019
Kidney	1.117 ± 0.133	0.312 ± 0.022	3.274 ± 0.565	0.883 ± 0.106
Adrenal gland	0.025 ± 0.004	0.005 ± 0.002	1.492 ± 0.186	0.323 ± 0.077
Pancreas	0.029 ± 0.001	0.017 ± 0.008	0.310 ± 0.012	0.140 ± 0.068
Spleen	0.029 ± 0.004	0.018 ± 0.002	0.203 ± 0.006	0.106 ± 0.020
Testis	0.014 ± 0.001	0.007 ± 0.001	0.079 ± 0.008	0.034 ± 0.003
Urine	2.816 ± 2.775	0.073 ± 0.060	40.66 ± 40.25	1.343 ± 0.439
Blood	0.051 ± 0.008	0.024 ± 0.011	0.102 ± 0.021	0.041 ± 0.017
Bone	0.052 ± 0.004	0.027 ± 0.003	0.161 ± 0.007	0.085 ± 0.009
Bone marrow	0.011 ± 0.003	0.003 ± 0.005	0.175 ± 0.082	0.025 ± 0.042
Muscle	0.051 ± 0.011	0.027 ± 0.004	0.061 ± 0.008	0.030 ± 0.001
Tumor	0.173 ± 0.029	0.092 ± 0.023	0.251 ± 0.010	0.097 ± 0.008
Excrement (urine)	88.87 ± 2.81	91.23 ± 13.05	NA	NA
Excrement (feces)	NA	2.102 ± 0.101	NA	NA

%ID = percentage injected dose; NA = not available.
Data are mean ± SE (n = 6).

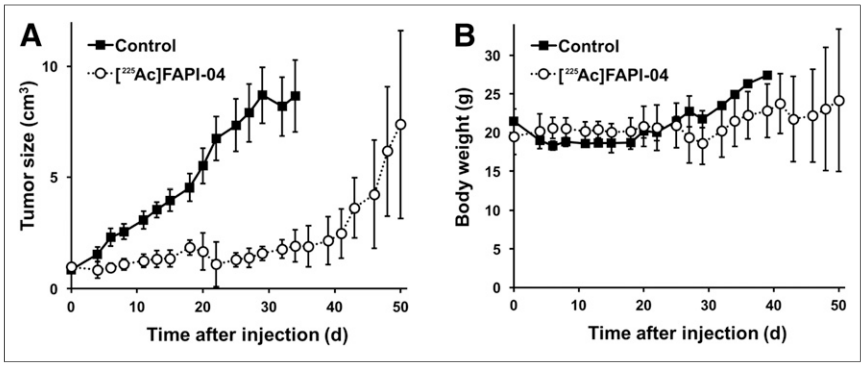

FIGURE 6. Treatment effect (A) and change in body weight (B) in PANC-1 xenograft mice after injection of ^{225}Ac-FAPI-04.

Here, we investigated subcutaneously implanted xenograft models rather than xenografts initiated by intrapancreatic implantation to measure tumor size over time using the caliper. Moreover, we used a relatively larger xenograft model, given that smaller tumors showed relatively lower expression of FAP (data not shown).

For the biodistribution of ^{64}Cu-FAPI-04 and ^{225}Ac-FAPI-04, a similar trend was observed in physiologic accumulation. It showed high accumulation in the liver and kidney, with a large amount of excretion observed in the urine and mild accumulation in the intestine. Rapid excretion through the kidney was also observed for ^{68}Ga-FAPI-04. The increased liver uptake of ^{64}Cu (Fig. 4) is most probably due to free radionuclides, because macrocyclic copper-chelates can suffer from limited in vivo stability against superoxide dismutase in the liver (*21*). Rylova et al. reported that ^{64}Cu-DOTATATE is more stable in humans than in mice (*22*). It is possible that ^{64}Cu- or ^{225}Ac-labeled FAPI-04 shows a different biodistribution in humans, especially for liver uptake. Regarding the kinetics of FAPI, relatively rapid washout from the tumor is a major problem during the use of FAPI-04 for radioligand therapy. FAPI compounds, such as FAPI-21 or -46, which exhibit improved tumor retention, should be used in future studies (*10*). Furthermore, for future studies, short–half-life isotopes, such as ^{211}At (7.2 h), would likely be optimal with FAPI; however, FAPI labeling with ^{211}At is currently technically difficult. Here, we only attempted to prove the concept that targeting FAP in cancer stroma with an α-emitter is effective.

The injected dose of ^{225}Ac-FAPI-04 in this study was 34 kBq per mouse. Based on body weight, this corresponds to a dose of 1.5 MBq/kg in humans (60 kg). Although this dose is relatively high as compared with ^{225}Ac-PSMA-617 therapy (50–200 kBq/kg), the optimal dose depends on ligand biodistribution and kinetics (*23*). In ^{225}Ac-FAPI-04 therapy, 89% of the injected dose was excreted in the urine at 3 h after injection because of the rapid kinetics of FAPI, resulting in a low residual amount of the ligand remaining in the body. We did not acquire images at later time points via ^{64}Cu-FAPI-04 PET (e.g., 24 or 48 h after injection), because of the limited experimental schedule. However, it is feasible to acquire these images to evaluate tracer kinetics and accurately calculate residence time for long–half-life radionuclides (^{64}Cu and ^{225}Ac). We observed no significant change in body weight after the administration of ^{225}Ac-FAPI-04, suggesting that it has minimal toxicity. For a more detailed evaluation of safety, hematologic or renal toxicity should be further investigated.

There are some limitations to the present study. We evaluated the treatment effect of a single dose (34 kBq) in only a PANC-1 model, because the supply of ^{225}Ac is very limited in Japan at the moment. Evaluations of dose dependency, optimization, and toxicity are still needed for the clinical application of α-therapy targeting FAP. We used in vitro cellular uptake analysis to confirm that FAP expression was not observed in the tumor cell itself. Although the lack of a positive control in the assay represents a limitation, it is possible that FAP expression can be observed in the xenograft (in vivo situation). FAP staining revealed a brown-stained area around the tumor cells, with some forming streaklike structures suggestive of fibroblasts exhibiting FAP expression. However, clear differentiation between stroma and cytoplasm or specific staining of the stroma is technically challenging work. Confirming the cellular specificity of FAP expression, as well as the effective mechanism of ^{225}Ac-FAPI-04 treatment, requires clarification in future work.

CONCLUSION

This study provided a proof of the concept that ^{64}Cu-FAPI-04 and ^{225}Ac-FAPI-04 can be used to treat FAP-expressing pancreatic cancer. α-therapy targeting FAP in the cancer stroma is effective and will contribute to the development of a new treatment strategy in combination with other therapies directly targeting cancer cells.

DISCLOSURE

This study was funded by the KAKENHI (B) (research number 19H03602) from the Ministry of Education, Culture, Sports, Science and Technology (MEXT) and by the QiSS program of the OPERA (grant JPMJOP1721) from the Japan Science and Technology Agency (JST). Uwe Haberkorn, Thomas Lindner, Clemens Kratochwil, and Frederik Giesel have a patent application for quinolone based FAP-targeting agents for imaging and therapy in nuclear medicine. Uwe Haberkorn, Thomas Lindner, Clemens Kratochwil, and Frederik Giesel also have shares of a consultancy-group for iTheranostics. No other potential conflict of interest relevant to this article was reported.

ACKNOWLEDGMENTS

We thank Takanori Kobayashi and Takashi Yoshimura for their excellent technical assistance. ^{225}Ac is provided by the ^{233}U cooperation project between JAEA and the Inter-University Cooperative Research Program of the Institute for Materials Research, Tohoku University (proposal 19K0053).

KEY POINTS

QUESTION: Is α-therapy targeting FAP in the tumor stroma effective for the treatment of pancreatic cancer?

PERTINENT FINDINGS: This study showed that ^{64}Cu-FAPI-04 and ^{225}Ac-FAPI-04 could be used in theranostics for the treatment of FAP-expressing pancreatic cancer. ^{225}Ac-FAPI-04 administration showed significant tumor growth suppression in the pancreatic cancer xenograft mice.

IMPLICATIONS FOR PATIENT CARE: α-therapy targeting FAP in the cancer stroma is effective and will contribute to the development of a new treatment strategy.

REFERENCES

1. Kratochwil C, Bruchertseifer F, Giesel FL, et al. ^{225}Ac-PSMA-617 for PSMA-targeted alpha-radiation therapy of metastatic castration-resistant prostate cancer. *J Nucl Med.* 2016;57:1941–1944.
2. Giesel FL, Knorr K, Spohn F, et al. Detection efficacy of ^{18}F-PSMA-1007 PET/CT in 251 patients with biochemical recurrence of prostate cancer after radical prostatectomy. *J Nucl Med.* 2019;60:362–368.
3. Xing F, Saidou J, Watabe K. Cancer associated fibroblasts (CAFs) in tumor microenvironment. *Front Biosci (Landmark Ed).* 2010;15:166–179.
4. Werb Z, Lu P. The role of stroma in tumor development. *Cancer J.* 2015;21:250–253.
5. Tao L, Huang G, Song H, Chen Y, Chen L. Cancer associated fibroblasts: an essential role in the tumor microenvironment. *Oncol Lett.* 2017;14:2611–2620.
6. Zi F, He J, He D, Li Y, Yang L, Cai Z. Fibroblast activation protein alpha in tumor microenvironment: recent progression and implications. *Mol Med Rep.* 2015;11:3203–3211.
7. Liu F, Qi L, Liu B, et al. Fibroblast activation protein overexpression and clinical implications in solid tumors: a meta-analysis. *PLoS One.* 2015;10:e0116683.
8. Loktev A, Lindner T, Mier W, et al. A new method for tumor imaging by targeting cancer associated fibroblasts. *J Nucl Med.* 2018;59:1423–1429.
9. Lindner T, Loktev A, Altmann A, et al. Development of quinoline-based theranostic ligands for the targeting of fibroblast activation protein. *J Nucl Med.* 2018;59:1415–1422.
10. Loktev A, Lindner T, Burger EM, et al. Development of fibroblast activation protein–targeted radiotracers with improved tumor retention. *J Nucl Med.* 2019;60:1421–1429.
11. Giesel FL, Kratochwil C, Lindner T, et al. ^{68}Ga-FAPI PET/CT: biodistribution and preliminary dosimetry estimate of 2 DOTA-containing FAP-targeting agents in patients with various cancers. *J Nucl Med.* 2019;60:386–392.
12. Kratochwil C, Flechsig P, Lindner T, et al. ^{68}Ga-FAPI PET/CT: tracer uptake in 28 different kinds of cancer. *J Nucl Med.* 2019;60:801–805.
13. Apostolidis C, Molinet R, Rasmussen G, Morgenstern A. Production of Ac-225 from Th-229 for targeted alpha therapy. *Anal Chem.* 2005;77:6288–6291.
14. Bao Q, Newport D, Chen M, Stout DB, Chatziioannou AF. Performance evaluation of the Inveon dedicated PET preclinical tomograph based on the NEMA NU-4 standards. *J Nucl Med.* 2009;50:401–408.
15. Spetz J, Rudqvist N, Forssell-Aronsson E. Biodistribution and dosimetry of free ^{211}At, ^{125}I- and ^{131}I- in rats. *Cancer Biother Radiopharm.* 2013;28:657–664.
16. Sathekge M, Bruchertseifer F, Vorster M, et al. Predictors of overall and disease free survival in metastatic castration-resistant prostate cancer patients receiving ^{225}Ac-PSMA-617 radioligand therapy. *J Nucl Med.* May 17, 2019 [Epub ahead of print].
17. Blakey DC, Westwood FR, Walker M, et al. Antitumor activity of the novel vascular targeting agent ZD6126 in a panel of tumor models. *Clin Cancer Res.* 2002;8:1974–1983.
18. Beloueche-Babari M, Jamin Y, Arunan V, et al. Acute tumour response to the MEK1/2 inhibitor selumetinib (AZD6244, ARRY-142886) evaluated by non-invasive diffusion-weighted MRI. *Br J Cancer.* 2013;109:1562–1569.
19. Gradiz R, Silva HC, Carvalho L, Botelho MF, Mota-Pinto A. MIA PaCa-2 and PANC-1: pancreas ductal adenocarcinoma cell lines with neuroendocrine differentiation and somatostatin receptors. *Sci Rep.* 2016;6:21648.
20. Lee HO, Mullins SR, Franco-Barraza J, Valianou M, Cukierman E, Cheng JD. FAP-overexpressing fibroblasts produce an extracellular matrix that enhances invasive velocity and directionality of pancreatic cancer cells. *BMC Cancer.* 2011;11:245.
21. Bass LA, Wang M, Welch MJ, Anderson CJ. In vivo transchelation of copper-64 from TETA-octreotide to superoxide dismutase in rat liver. *Bioconjug Chem.* 2000;11:527–532.
22. Rylova SN, Stoykow C, Del Pozzo L, et al. The somatostatin receptor 2 antagonist ^{64}Cu-NODAGA-JR11 outperforms ^{64}Cu-DOTA-TATE in a mouse xenograft model. *PLoS One.* 2018;13:e0195802.
23. Kratochwil C, Bruchertseifer F, Rathke H, et al. Targeted alpha-therapy of metastatic castration-resistant prostate cancer with ^{225}Ac-PSMA-617: dosimetry estimate and empiric dose finding. *J Nucl Med.* 2017;58:1624–1631.